Novel concept for large deformable mirrors

T. Andersen
O. Garpinger
M. Owner-Petersen
F. Bjoorn
R. Svahn
A. Ardeberg
Lund Observatory
Box 43
SE-221 00 Lund, Sweden

Abstract. Large, high-bandwidth deformable mirrors (DMs) with thousands of actuators for adaptive optics are of high interest for existing large telescopes and indispensable for construction of efficient future extremely large telescopes. Different actuation and sensing principles are possible. We propose a novel concept using commercially available voice coil actuators attached to the back of the mirror with suction cups and using LVDT sensors on the actuators for local stabilization. Also, a new low-cost sensor for easy measurement of DM displacement or velocity has been developed. It has a sensitivity better than 20 nm and a bandwidth wider than 20 to 1000 Hz. Finally, studies are in progress of global, hierarchical mirror form controllers based on many parallel multiple-input, multiple-output regulators of low order. © *2006 Society of Photo-Optical Instrumentation Engineers.* [DOI: 10.1117/1.2227014]

Subject terms: mirrors; actuators; adaptive optics; active optics; wavefront compensation; telescopes.

Paper 050504RR received Jun. 26, 2005; revised manuscript received Dec. 23, 2005; accepted for publication Dec. 28, 2005; published online Jul. 26, 2006.

1 Introduction

In modern optical telescopes, adaptive optics correct for static and dynamic aberrations from the atmosphere and the telescope. Adaptive optics have deformable mirrors (DMs) whose form can be adjusted in real time under computer control. Traditionally, DMs have been small (10 to 30 mm), because it is much easier to achieve a high temporal bandwidth with a small mirror than with a large. However, as first proposed by Jacques Beckers in 1989,[1] for large optical telescopes it is preferable to integrate the adaptive optics into the telescope, making one telescope mirror (typically the secondary) deformable. This way, lossy relay optics is avoided and the telescope system becomes more compact. This is particularly true for the planned generation of extremely large telescopes (ELTs) currently being designed by several groups worldwide. For reasons of light efficiency and laser beacon imaging, availability of DMs in the 2- to 4-m class is in practice imperative for successful design of ELTs. The possibility of constructing ELTs with deformable primary mirrors has also been discussed.[2]

Only a few DMs exist. A 64-cm DM of Zerodur has been successfully implemented on the upgraded Multi-Mirror Telescope (MMT)[3,4] using electromagnetic force actuators glued to the back of the mirror and a 40-μm air gap for damping between the mirror and a backing structure. A larger mirror (91 cm), following roughly the same design principles but without aerodynamic damping, is now being installed on the Large Binocular Telescope.[4] For that mirror, adequate damping is obtained through a special design of the actuator servos. A study of a control system for a DM using circulant matrices and taking the atmospheric noise properties into account has also been carried out.[5,6] Finally, a group is working on development of deformable carbon-fiber-reinforced mirrors using magnetostrictive actuators.[7–9]

Related to studies of an ELT with a primary mirror diameter of 50 m (the Euro50) at Lund Observatory,[10] a conceptual design of a 4-m DM has been undertaken and an actuator test stand built. Here we report on the progress of that work. Although the development work was done within the framework of the Euro50 project, the results are applicable to any large DM.

2 Overview and Requirements

Actuators exert forces on a thin faceplate to deform it into the shape commanded. The mirror shape is detected by the wavefront sensor of the complete adaptive optics system. For stabilization, additional local feedback of the mirror velocity or position is also necessary, using sensors on the back of the mirror. Depending on the system design, this may be used for mirror *"flattening"* as well. For K-band observations ($\approx$2.2 μm), a 3.84-m DM for a 50-m ELT will have 3168 actuators and up to several thousand velocity or position feedback sensors on the back of the mirror.

The few large DMs now existing were made of glass or glass ceramics, attractive for mirrors in the 1-m class. However, the handling risk of a 4-m mirror with a thickness of about 2 mm is high. Also, polishing such a faceplate is challenging, and it is risky to make a polishing investment in a single 2-mm faceplate. Faceplates can also be fabricated using carbon-fiber-reinforced polymer (CFRP) layup directly on a mandrel.[11,12] Although the technique is not finally documented for large mirrors for visible wavelengths, there is evidence that it will be applicable to DMs for the K band, the wavelength aimed at for early ELT operation. From a systems point of view, it is preferable that large DMs have a concave form. Because of the complexity, deformable mirrors must be easy to test in situ, and such a test is most easily accomplished at the conic foci of a concave mirror.

Different types of actuators are possible, and they fall into two groups: Stiff actuators (*position actuators*) estab-

lish a stiff connection between the backing structure and the faceplate. Examples are magnetostrictive and piezoelectric actuators. They must typically be glued to the back of the mirror and attached to the backing structure with very strict tolerances. Any dimensional error in the process will be cast into the system for good. A position actuator that is not working will typically produce a bump at its location. With the large number of actuators, it is likely that there will always be actuators out of order. The magnetostrictive actuators often have high heat dissipation. The major advantage of the position actuators is that they are easy to handle from a servo point of view because the resonant frequencies are outside the operating range.

The resilient actuators (*force actuators*) used so far for large DMs have been of the electromagnetic type (voice coil) with a coil in the magnetic field of a permanent magnet. These actuators do not establish a physical connection between the faceplate and the backing structure, so they are simpler to assemble and service, and the tolerances are not as strict as for the position actuators. They have the advantage that they do not influence the mirror form when they are switched off due to malfunctions. The main problem with this type of actuator is related to the difficulty of establishing stable, high-bandwidth servos without cross-coupling between adjacent actuators through the mirror. Also, pure voice coil actuators must have a stiff connection to the faceplate and yet add as little mass to it as possible. Finally, there is a packing problem because the voice coils used so far take up some space and, in some cases, cannot be packed closely enough for visible-light observations.

It has lately become clear that adaptive optics for ELTs must correct not only for atmospheric aberrations but also for telescope aberrations due to wind, gravity, and system noise. In fact, there is evidence that the corrective effort for the latter may be harder than for the atmosphere. The dynamic range needed to correct for the atmosphere is around 3 to 5 μm,[10] whereas integrated modeling[13,14] shows that it may be greater than 20 μm for telescope aberrations. Not only does this preclude the use of micro-opto-electromechanical systems (MOEMS) as the sole corrective element, but it also strongly favors voice coil actuators. A significant fringe benefit is that because the actuators can handle a large range, the DM can also perform a tip-tilt correction, avoiding the need for a fast, separate tip-tilt mirror (although a slow one may still be needed).

Based on this, the following requirements can be formulated:

- Successful *actuators* must have a stroke of at least 20 μm, a force capability of ±2 N (as determined from a finite element model), a spacing down to 20 mm (defined by Fried's parameter at 500-nm wavelength), and a bandwidth well above 1 kHz (to achieve a global bandwidth of 500 to 1000 Hz). In addition, the sensors should be capable of absorbing mounting tolerances perpendicular to the mirror of 1 to 2 mm, no part should be glued to the back of the DM, the heat dissipation should be sufficiently low not to require external cooling, it should be quickly plug-in replaceable, and the cost should be low.
- Successful *sensors* should have a noise level below 50 nm (for K-band operation), have a bandwidth from below 20 Hz to well above 1 kHz, and be capable of absorbing mounting tolerances perpendicular to the mirror of 1 to 2 mm. Also, they should have low cost and be compatible with an actuator spacing down to 20 mm.
- Calculations that have been confirmed by simulations with an integrated model[10] show that the *global control system* for the mirror should have a closed-loop bandwidth of at least 500 Hz (preferably higher) to achieve a Strehl ratio of 0.4 for an ELT. Further, the control concept should be applicable for future DMs with 20,000 to 100,000 actuators.

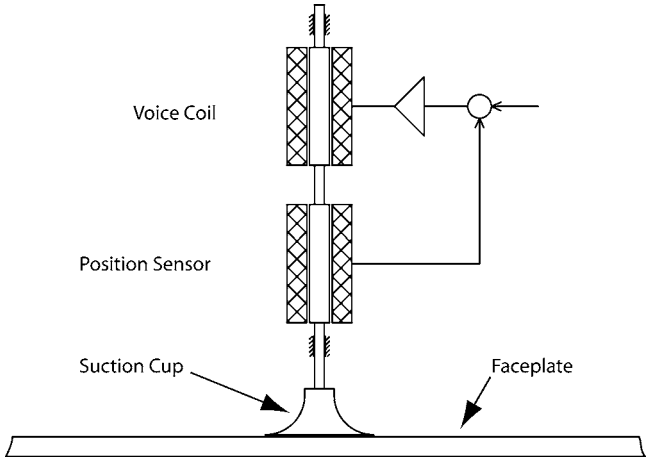

Fig. 1 Actuator concept.

None of the existing systems fulfill these requirements. In this article, we describe a concept for a system that (with minor adaptations) does so with a cost per actuator of about $800 and per sensor of $10, both including electronics. Existing systems based on voice coils and capacitive sensors are more expensive, not the least because they involve expensive and risky gluing of thousands of parts to the back of the mirror with a tolerance of some 10 to 50 μm. With our design there are no parts to be glued.

Further, systems already built have air gaps of the order of 200 μm (voice coils) and 50 μm (capacitive sensors). Consequently the tolerances of the matching parts must be very small, and hence the system will be costly to manufacture. The actuators and sensors of our system can absorb manufacturing tolerances of 1 to 2 mm. For existing systems, dust contamination is critical, because particles in the 50-μm air gap may be detrimental to system performance. For our system, dust is hardly an issue.

We are also proposing a hierarchical controller for the complete system using local controllers grouped in overlapping families that are largely decoupled from each other. Studies seem to suggest that this system has a higher bandwidth than existing systems. Work is still in progress on this issue.

3 Conceptual Design

The actuator concept with a commercially available voice coil is shown in Fig. 1. To provide easy attachment to the back of the mirror, convenient manufacturing tolerances, and simple exchange of faulty actuators, a suction cup is

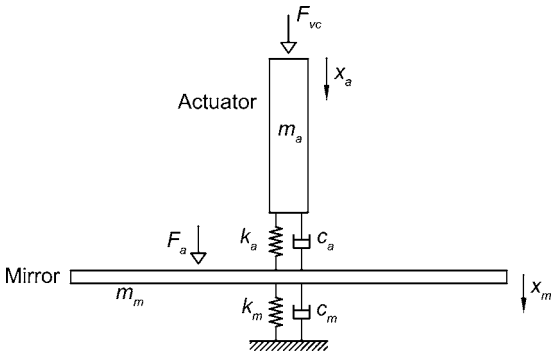

Fig. 2 Graphical illustration of a mathematical model of an actuator and part of the faceplate. Here x_a is the displacement of the actuator rod, x_m the displacement of the mirror at the location of the actuator, F_{vc} the voice coil force, F_a the force exerted on the mirror, m_a the mass of the actuator rod, m_m a lumped mass of a representative part of the mirror, k_a the stiffness of the suction cup, k_m the stiffness of the lumped-mirror-mass connection to the rest of the mirror, c_a the viscous damping coefficient of the suction cup, and c_m the viscous damping coefficient of the connection between the lumped mirror mass and the rest of the mirror.

used. The suction cup is evacuated through a thin hose (not shown). The entire DM may be easily disconnected by simply switching off the vacuum system.

The rim of the inner hole is fixed to the backing support structure. The back of the mirror is smooth, and there is no need to glue any parts onto it or to machine fixation surfaces and holes. A safety clamp holds the mirror in case of a malfunction of the vacuum system.

The suction cup is a soft structural member, and resilience between the voice coil and the mirror is in principle undesirable because it adds a new low-frequency eigenmode, largely defined by the mass of the actuator rod and the stiffness of the suction cup. To circumvent this problem, a position sensor is used as shown in Fig. 1. A mechanical model of the proposed system is shown in Fig. 2. The sensor is of the linear variable differential transformer (LVDT) type, which is highly reliable and inexpensive. The feedback signal from the LVDT is used in a servo system that controls the position of the actuator rod with a precision of a few microns. The force acting on the faceplate is proportional to the difference between the position of the actuator rod and the faceplate deflection. Tuning the spring constant of the suction cup appropriately, the movement of the actuator rod will generally be larger than the deflection of the faceplate by more than an order of magnitude, so the requirements on the precision of the LVDT are not nearly as strict as for the position sensing of the mirror itself. The servo system forces the actuator to move with a bandwidth of more than 1 kHz, and the force exerted on the mirror is largely proportional to the excursion of the actuator rod. More information on actuators is given in Sec. 4.2.

At first glance, it may seem that information from a wavefront sensor at the final telescope focus of an ELT could suffice for control of the entire telescope, including adaptive optics. The wavefront sensor indeed gives the ultimate information on the image quality. However, studies with an integrated simulation model[15] reveal that to suppress the influence of disturbances and noise sources, a variety of other sensors are also needed throughout the telescope system. For the large DMs of an ELT, internal position or velocity sensors are needed for global control of the DM for stabilization and noise suppression.

The proposed DM (faceplate) of the Euro50 is hexagonal, concave, and made of a CFRP in a replication process. The mirror is fabricated using CFRP layup on a mandrel, using an appropriate agent to ease separation of the DM from the mandrel. Suppression of fiber print-through on the reflecting surface is of importance. High-quality fibers must be used to obtain a stiff and thin mirror. More information can be found in Ref. 11.

The thickness of the mirror must be chosen as a compromise. Basically, the mirror should be as thin as possible to permit small actuation forces to produce large excursions. However, it should be thick enough to prevent excessive gravity sag between the supports. With the present carbon fiber layup and actuator geometry, a thickness of 2 mm is required to keep the total gravity errors below 25 nm rms (for the K-band mirror).

The global control system should work at a bandwidth of at least 500 Hz (target 1 kHz) and limit the maximum global rms error to 80 nm for the K band. Due to the large size of the Euro50 mirror, there are more than 800 poorly damped eigenmodes that can be excited within the bandwidth of the control system. Very few (if any) standard approaches are available for control of a heavy coupled multiple-input multiple-output (MIMO) system of this nature. We propose a hierarchical system with multiple MIMO regulators working in parallel. More information can be found in Sec. 6.

Because force actuators are used, the structure behind the mirror does not influence the dynamics or precision much. The absolute precision is defined by the external wavefront sensor. Only at frequencies above 20 Hz does the stability of the underlying structure play a role. Hence, the structure need not be thermally highly stable, so a CFRP structure will suffice. The weight of the movable part of the actuator is small compared to that of the relevant part of the mirror mass and can be compensated by a current proportional to the sine of the altitude pointing angle of the telescope. The cables are fixed to the backing structure. Hence, neither the weight of actuators nor that of cables will influence the mirror in any way.

4 Actuators

The actuator proposed has an internal servo loop to establish a band that is higher than the eigenfrequency defined by the mass of the moving part of the actuator and the suction cup. In the following, the principle is further described using a simulation model, and a prototype design is presented together with laboratory test results.

4.1 *Mathematical Models*

A graphical illustration of a simple mathematical model of the actuator and the mirror, with symbol definitions, is shown in Fig. 2. Two masses represent the moving actuator rod and a part of the faceplate. The equivalent faceplate stiffness k_m, represented by a spring connection to ground, has been carried over from a local finite element model of the faceplate, but in reality the faceplate is a complex dynamic structure. The spring connecting the actuator rod and the faceplate, k_a, represents the suction cup and is tunable

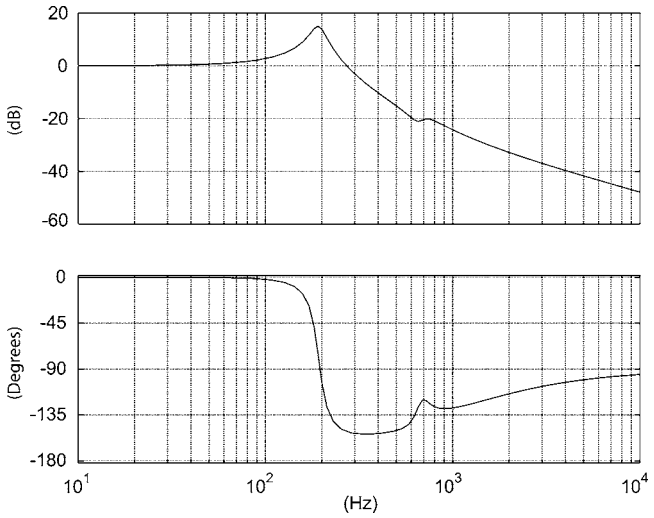

Fig. 3 Bode plot of transfer function from the voice coil force F_{vc} to the force acting on the faceplate, F_a.

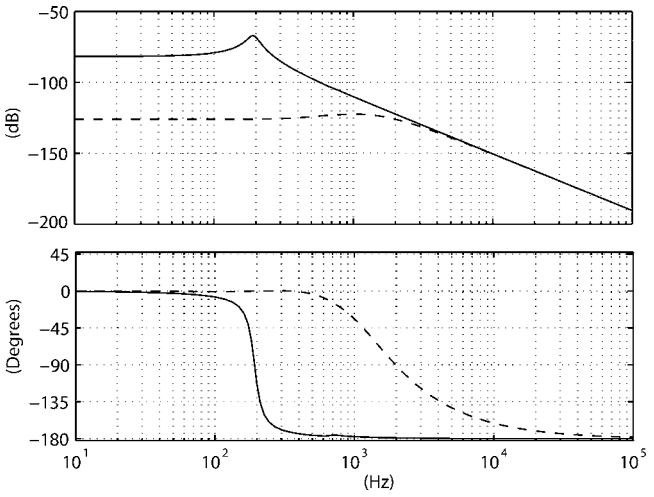

Fig. 4 Solid curve: transfer function from voice coil force, F_{vc}, to actuator displacement. Dashed curve: closed-loop transfer function from actuator rod displacement command, x_r, to actuator rod displacement, x_a.

by design within limits. The damping ratios for suction cup and faceplate have been assumed to have the value 0.1.

Figure 3 shows the transfer function from the force generated by the voice coil, F_{vc}, to the force exerted on the back of the DM, F_a, without any internal feedback in the actuator. Not surprisingly, the actuator works well at low frequencies, but there is a cutoff frequency set by the spring constant k_a of the suction cup and the mass m_a of the moving actuator rod. The effect of the inductance of the voice coil is small and can be suppressed by an appropriate current loop, so it is not taken into account here. The upper curve of Fig. 4 is the open-loop transfer function, x_a/F_{vc}, which is very similar to that of Fig. 3, since the movement, x_a, of the actuator rod is much larger than the deflection, x_m, of the faceplate for this choice of parameters. Below the cutoff frequency, the amplitude is determined by the spring constant of the suction cup, k_a, and above, by the inertia of the actuator rod. A servo loop with feedback from the LVDT position sensor in the actuator is then added to increase the bandwidth. The lower curve of the same figure shows the closed-loop performance with appropriate scaling. A proportional-integral (PI) controller with a corner frequency of about 200 Hz has been used in conjunction with lead compensation at the crossover frequency (1.4 kHz) to achieve an appropriate phase margin. This is necessary because the LVDT measures position and not velocity. It can be seen that the effect of the LVDT loop is to remove the poorly damped resonance defined by the suction cup and the mass of the actuator rod, and establish a higher cutoff frequency of the actuator.

The model just presented, with a PI controller and lead compensation, is highly useful for understanding the operating principle of the actuator. In practice, however, noise and crosstalk call for use of a somewhat different controller. The lead compensation described increases the gain at high frequencies, thereby amplifying crosstalk from actuator input to LVDT output and noise in the range 1 to 10 kHz. Measurements show this to be critical, so instead an observer-based controller is used. Figure 5 shows the principle. The observer, shown in the lower part of the figure, serves as an analog computer receiving the same input as the real actuator and computing the position of the actuator rod. Using a PID controller, the observer is slaved to follow the actual position measured by the LVDT. To avoid noise amplification, the differential component of the controller is implemented by a feedforward bypass of the first integrator of the observer.[16] The observer directly provides velocity and position signals for the actuator control loops. Use of the observer corresponds to working closed-loop up to a frequency around 200 Hz, and open-loop between 200 Hz and 1.4 kHz.

It is important that the heat dissipation of the actuators be low. In ELTs, correction must be made both for atmospheric aberrations and for aberrations due to telescope misalignment, in particular due to wind. The wind-induced aberrations are large, typically up to 20 μm, but somewhat slower than the atmospheric aberrations. Heat dissipation is most critical for higher frequencies, above the actuator-rod-mass resonant frequency set by the suction-cup spring. Thus, as a realistic and conservative scenario, the heat dissipation from the Ohmic losses in the voice coil for atmospheric corrections has been estimated using a Simulink model.

The von Kármán spatial power spectrum for the phase[17] is given by

$$\mathrm{PS}_{\varphi}(f_s) = 0.0229 \frac{1}{r_0^{5/3}} \left(f_s^2 + \frac{1}{L_0^2} \right)^{-11/6},$$

where f_s is the magnitude of the two-dimensional spatial frequency, r_0 is Fried's parameter, and L_0 is the outer scale of the atmosphere. Approximating the temporal frequency f as

$$f = v_e f_s,$$

where v_e is the effective air speed, gives the temporal power spectrum for the phase,

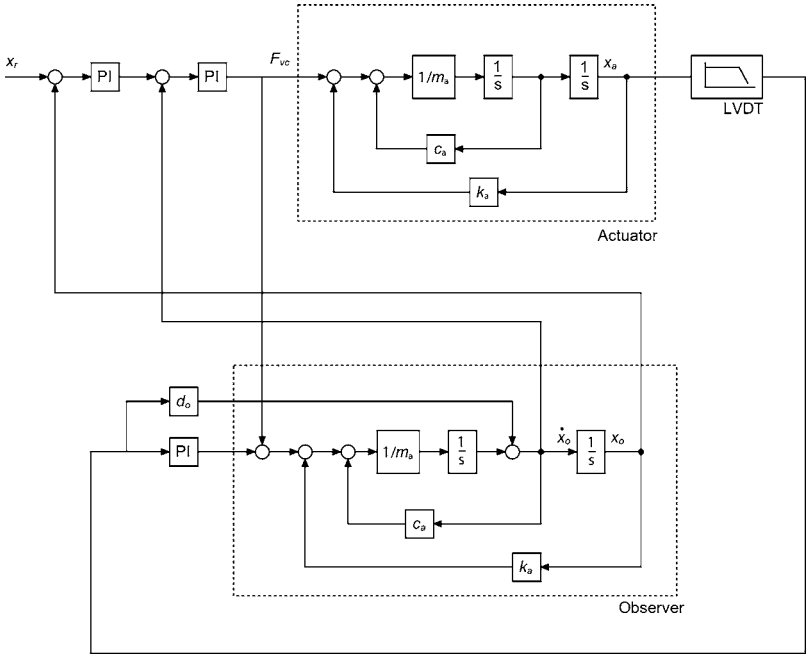

Fig. 5 Principle of observer-based controller for the actuator.

$$P_{\varphi}(f) = 2\pi \frac{f}{v_e^2} \mathrm{PS}_{\varphi}\left(\frac{f}{v_e}\right).$$

An estimate of the power spectral density (PSD) for the stroke of a single actuator is then given by

$$P_{x_m}(f) = P_{\varphi}(f)\left(\frac{\lambda}{4\pi}\right)^2 = 9.15 \times 10^{-4} \times \lambda^2 \left(\frac{v_e}{r_0}\right)^{5/3} f\left[f^2 + \left(\frac{v_e}{L_0}\right)^2\right]^{-11/6},$$

where λ is the wavelength. This estimate is conservative in that the average stroke over all actuators is not subtracted. Approximating the DM with a second-order system, the transfer function from the force exerted on the back of the mirror, F_a, to the deflection of the faceplate, x_m, becomes

$$F_f(s) = \frac{x_m(s)}{F_a(s)} = \frac{1/k_m}{\frac{s^2}{\omega_n^2} + 2\zeta\frac{s}{\omega_n} + 1}.$$

Here, ω_n is the eigenfrequency of the mirror mode taken into account (660 Hz), and ζ the corresponding damping ratio of 0.1. Hence, the PSD of the force on the mirror is

$$P_{F_a}(f) = \frac{P_{x_m}(f)}{|F_f(j2\pi f)|^2}.$$

A sample time series with this PSD is shown in Fig. 6 (top) together with the corresponding heat dissipation (bottom). The average power dissipated is 34 mW per actuator, conveniently low. For a large DM, as for the Euro50 with 3168 actuators, some forced cooling is desirable to suppress heat leakage to the ambient air. The heat dissipation depends only weakly on L_0, for the heat-generating mechanism is mainly related to moving the actuator rod quickly in the 200- to 1000-Hz range. The model is somewhat conservative in that the low-frequency forces are exaggerated.

4.2 *Prototype Design*

A prototype of an actuator with a mirror simulator was tested in the laboratory. The actuator prototype is shown in Fig. 7, and the test setup in Fig. 8. The driving electronics is analog. The final system will likely have a combination of analog and digital circuitry.

The mechanical parts are of brass to minimize magnetic coupling. A magnetic shield between the voice coil and the LVDT was tested but only a small effect on cross talk between the voice coil and the LVDT was found. The prototype actuator is fixed to the base plate with a flange. In the final units, a bayonet fixation will be used to allow closer packing and easy exchange of actuators. The voice coil is of a commercial type. The linear bearings for the actuator

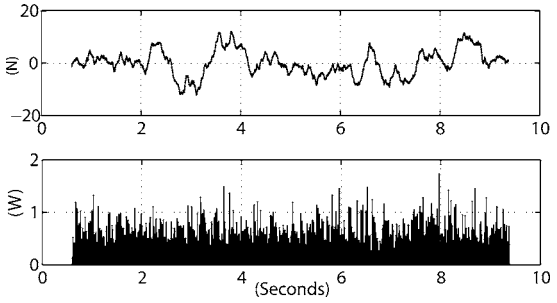

Fig. 6 Upper curve: time series showing a typical force command signal over time. Lower curve: time series of heat dissipation in actuator. Here L_0=25 m, v_e=15 m/s, λ=2.2 μm, r_0=1 m, $\omega_n = 2\pi \times 660\ \mathrm{s}^{-1}$, ζ=0.1, and $k_m = 1.72 \times 10^5$ N/m.

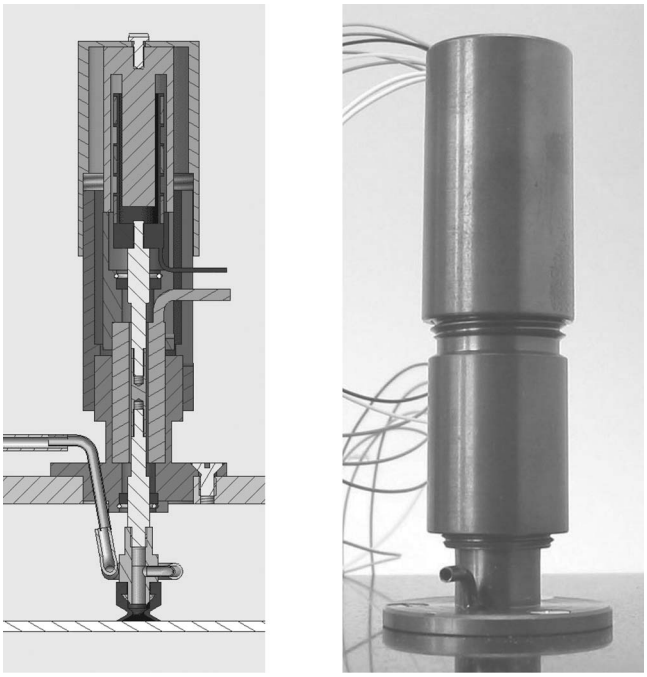

Fig. 7 Actuator prototype.

rod are of Teflon. The suction cup is commercially available and is actually stiffer than desired, so an additional resilient rubber element was introduced. This also reduces transverse forces to a negligible level. Vacuum in the suction cup is established with an external pump.

A block diagram of the prototype electronics is shown in Fig. 9. The LVDT circuitry includes a sine wave driver and a synchronous detector with appropriate filters. The peak rating of the voice coil is much higher than the average rating, so a thermal protection circuit has been designed (although not yet implemented). The power amplifier has a current limit to be set at the peak rating of the voice coil,

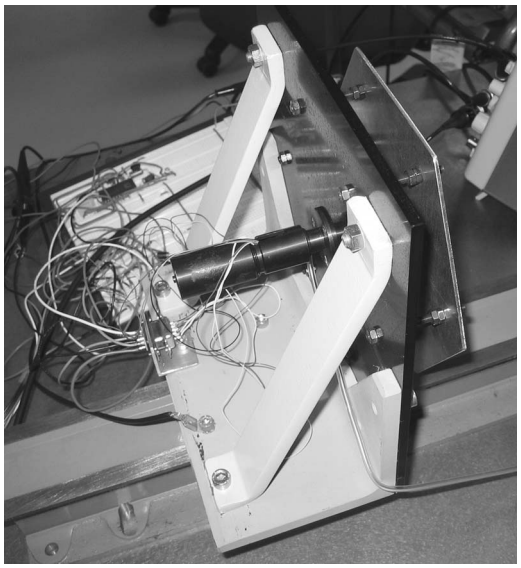

Fig. 8 Laboratory test stand with actuator and mirror simulator.

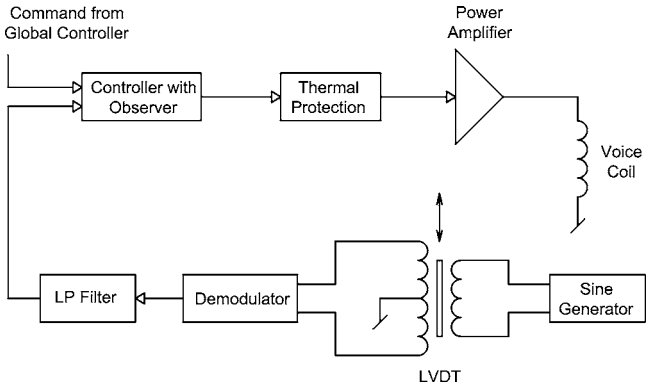

Fig. 9 Block diagram of prototype electronics.

4.2 N. The observer and the controllers were implemented with operational amplifiers. Electronic circuits were simulated beforehand in PSPICE to validate their performance against Simulink simulations.

4.3 *Prototype Performance*

The prototype actuator and electronics were tested in the laboratory. The faceplate of the final Euro50 secondary mirror will be made of CFRP, but for the test stand, a plane, 2-mm aluminum dummy with a similar stiffness was used. It was supported in six points at the location of the adjacent actuators for the true mirror faceplate. Mirror deflection was studied with the position sensors described in Sec. 5 and a laser velocimeter.

Figure 10 shows the measured transfer function from the position input (normally coming from the LVDT) to the estimated observer position. As expected, the observer re-

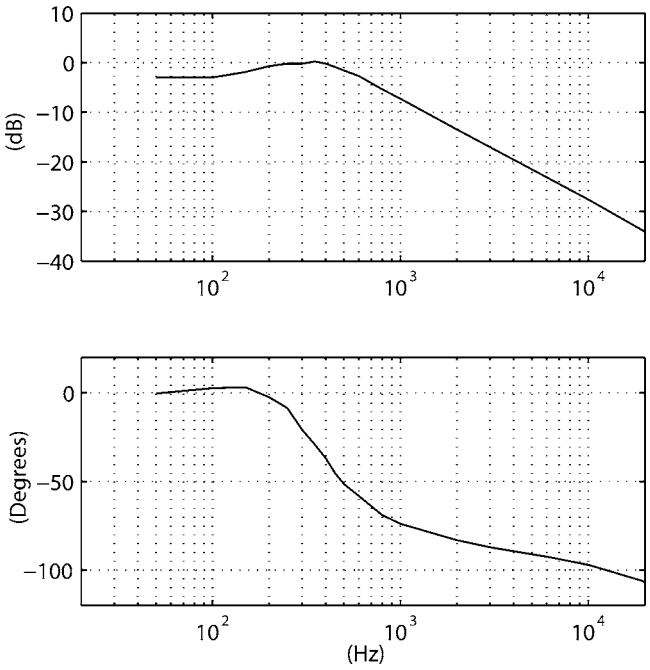

Fig. 10 Measured transfer function from position of the linear variable differential transformer (LVDT) to position estimated by observer.

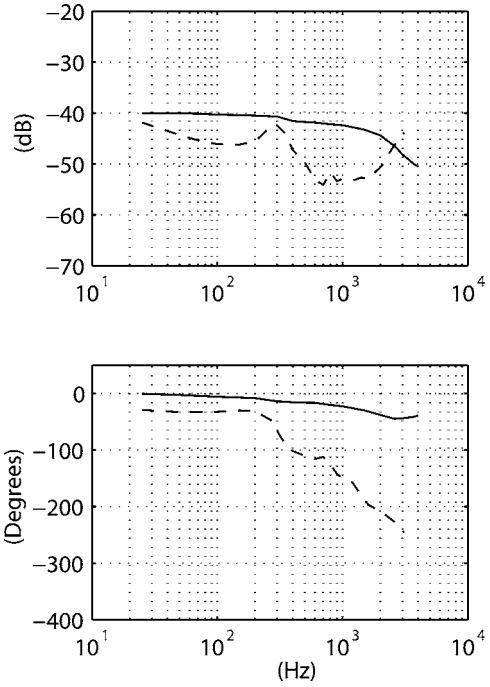

Fig. 11 Closed-loop performance of complete actuator with position command taken as input and observer position estimate (full line) and LVDT position measurement (dashed) as output.

lies on the LVDT input up to a cutoff frequency of some hundred Hertz. Above this value, the observer position is determined open-loop by the driving input to the voice coil.

The closed-loop performance of the complete actuator is seen in the Bode plots of Fig. 11. The input is the actuator position command (largely corresponding to the force due to the soft suction cup), and the output is the observer estimate of position (solid lines). The dashed lines of the same figure show a similar curve, but here the measured LVDT signal is taken as output instead. Apart from a small dc gain difference also apparent in Fig. 10, the LVDT output stays within ±3 dB up to some hundred Hertz, above which it first drops off as expected. At higher frequencies, it increases again due to crosstalk, and it is in fact the wish to discriminate this crosstalk that has led to the use of an observer.

Sensitivity of the final system to LVDT noise is an important issue. Figure 12 shows the measured PSD of the LVDT position signal, $P_{\mathrm{LVDT}}(f)$, when the rest of the system is switched off. The standard deviation of the LVDT noise is 128 nm.

The purpose of the internal LVDT loop is to stabilize the actuator. There will be at least two additional control loops around the DM, using feedback signals from the position/deformation sensors on the faceplate and from the wavefront sensors. Hence, LVDT noise will be suppressed by the external loops, and the precision needed for the LVDT is much less than for the position sensors of the DM or the wavefront sensor. To get insight into the influence of LVDT noise on the final system, external velocity and position control loops for the faceplate were implemented in a simulation model using PI controllers with bandwidths of 1.8 and 1.4 kHz, respectively. The Bode plot for the corresponding LVDT-noise to mirror-displacement transfer function, $F_{\mathrm{LVDT}}(s)$, is shown in Fig. 13. The resulting noise spectrum for mirror excursions is

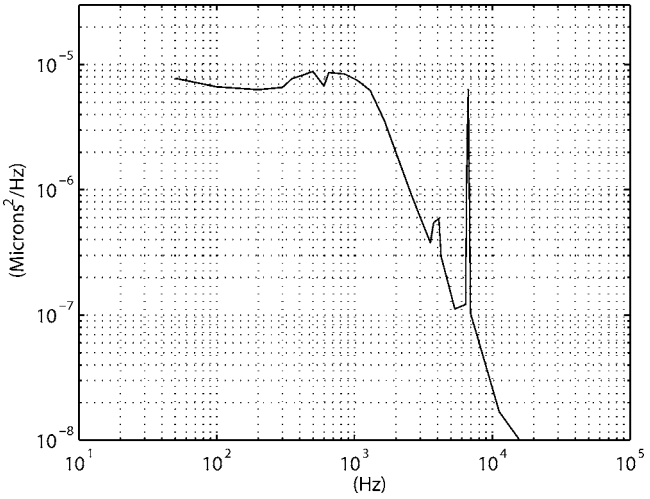

Fig. 12 Power spectral density of LVDT sensor noise.

$$P_{x_m}(f) = |F_{\mathrm{LVDT}}(i2\pi f)|^2 P_{\mathrm{LVDT}}(f),$$

as shown in Fig. 14. The corresponding standard deviation of the mirror displacement noise is 0.6 nm, which is negligible in this context. If there were uncontrolled resonances near the cutoff frequency of the mirror controller, that would increase the value, but there is sufficient margin to handle this. Also, it is likely that the LVDT noise can be reduced even further through a more careful design of the LVDT electronics. In conclusion, LVDT noise will not pose problems for the overall control of the DM.

It would be possible to measure the position of the simulator mirror and establish closed-loop control of the mirror position in the test stand. This would require shaping of various bandpass filters specific to the actual test setup and

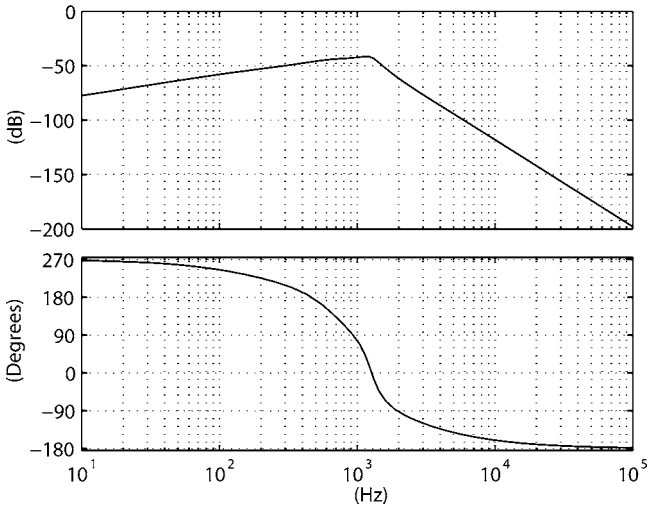

Fig. 13 LVDT-noise to mirror-displacement transfer function with tentative controller.

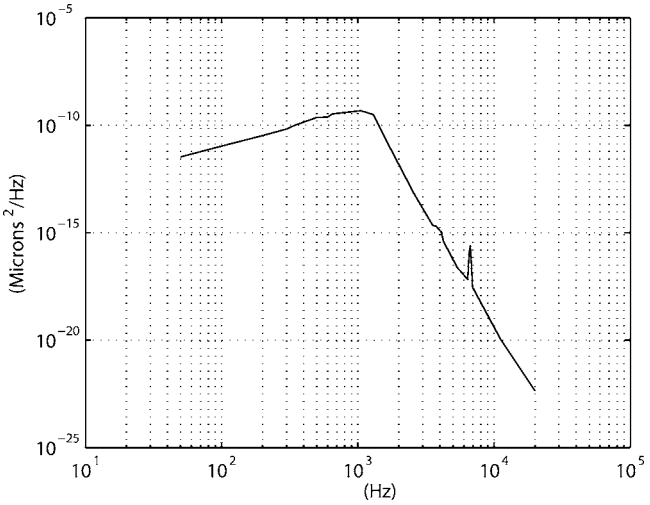

Fig. 14 Estimate of mirror noise PSD due to LVDT sensor noise.

not to the concept. Thus, we decided not to implement such a test system, but await tests with a 7- or 19-actuator mirror.

5 Sensors

Internal position and/or velocity sensors are needed for stabilization and noise suppression. Due to the availability of an external reference signal from the wavefront sensor, a measurement in the frequency range 20 to 1000 Hz will suffice. It is, however, important that the sensor accommodate a dynamic range from less than 50 nm (for K-band adaptive optics) and up to 20 μm. It is also essential that the sensor accept large installation tolerances (1 to 2 mm) to keep the manufacturing cost of the DM unit manageable.

A new type of sensor fulfilling these requirements has been developed.[18] It is based on an electret microphone with a cost of about a dollar. It has a flat frequency response from 20 Hz to 16 kHz, covering the frequency range of interest for our sensor application. There is no need for expensive preamplifiers or special signal-conditioning units. Electret microphones have been miniaturized and are available with diameters of a few millimeters.

The sensor is shown in Fig. 15. The electret microphone is supported by the backing structure and is fitted with rubber bellows that attach to the microphone at one end and touch the mirror at the other end with a small preload to keep the connection airtight. The backing structure must be

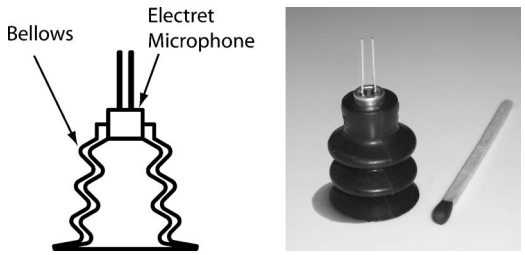

Fig. 15 Displacement sensor. Left: principle. Right: photo of prototype.

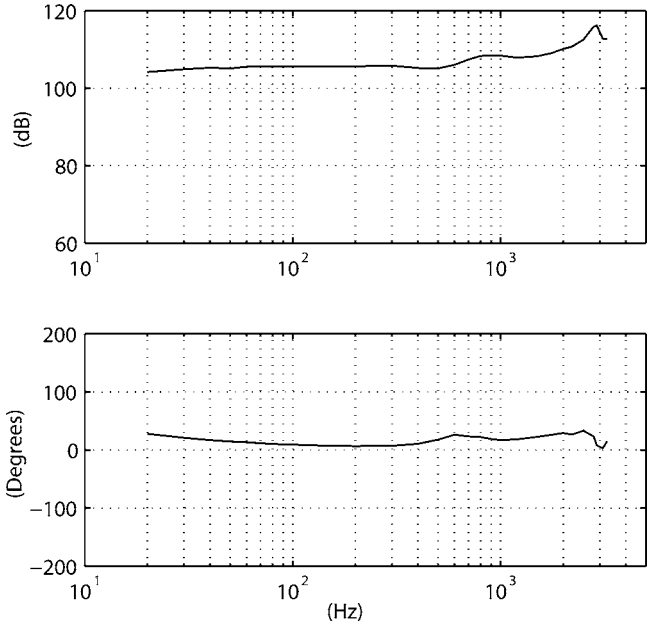

Fig. 16 Transfer function for displacement sensor, from faceplate deflection, x_m, to electret microphone voltage, V_m.

sufficiently rigid to suppress structural coupling between actuators and sensors. The preload on the mirror is negligible in a local perspective, and globally it can easily be corrected by the actuators. A microphone is a pressure sensor, and the bellows establish an internal pressure proportional to the movement of the DM. The bellows thus form a pressure chamber, increasing the sensitivity of the microphone to mirror movements as compared to placing the microphone alone in front of the mirror. The bellows also reduce the sensitivity to external acoustic noise to a negligible level.

The sensor was tested on a vibration table, using a sensitive accelerometer to record displacement. The measured transfer function is shown in Fig. 16. The sensor has a flat response (±2 dB) from the lower cutoff of the microphone at 20 Hz to about 1.5 kHz. Below 20 Hz it rolls off with 20 dB/decade. In the range 30 to 600 Hz it is within ±1 dB. It is not known whether high-frequency effects seen at 3 to 5 kHz stem from the sensor or the measurement setup, but it will be straightforward to establish a low pass cut off filter at about 1 kHz.

Figure 17 shows that the linearity of the device is good, better than 2.4%. With the present scaling of the driving circuit for the microphone, the dynamic range is from about 20 nm to nearly 5 μm. A larger measurement range is achievable through other component choices. Also, it is possible to measure deflections even smaller than 20 nm with the sensor, provided that careful grounding and shielding techniques are applied. Figure 18 shows the measured PSD of the sensor noise. The standard deviation of the noise over the range 0 to 1 kHz is 3.1 nm.

The sensitivity to acoustic noise was found to be below the acoustic pickup by the faceplate. Bellow vibration may ultimately limit sensor performance, so it is essential that the bellows be longitudinally as symmetrical as possible to reduce internal pressure variations due to bellow vibrations.

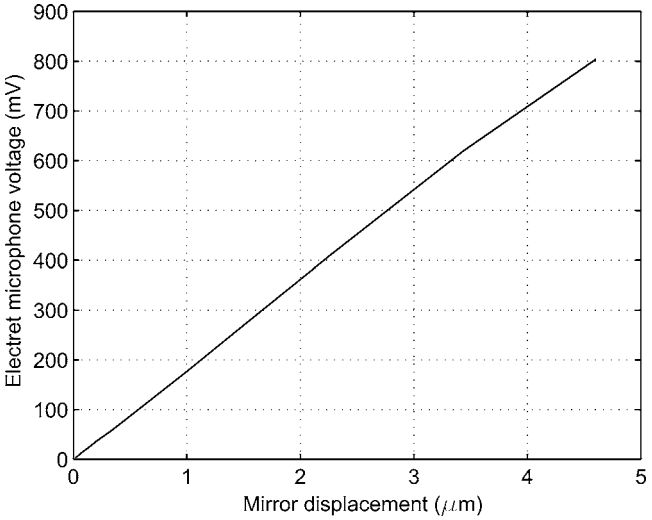

Fig. 17 Linearity of sensor measured at 500 Hz.

No attempt was made to optimize the bellows at this time, and an even wider bandwidth and dynamic range seem attainable through careful design of the bellows.

The sensor presented measures displacements. It is an interesting possibility to convert it into a velocity sensor by introducing a hole in the bellows. The size of the hole would define the transition frequency below which the sensor serves as a velocity sensor and above which it is a position sensor. Tuning the size of the hole appropriately (possibly using a capillary tube), a velocity sensor with a bandwidth of 1 to 2 kHz should be achievable. The hole will make the sensor more sensitive to acoustic noise, but that problem may possibly be solved by venting the hole to a large, closed reservoir. This approach has not been studied in detail.

Tests of the effect of a hole in the bellows were made, and some results are shown in Fig. 19. At low frequencies, the effect is as expected. However, a poorly damped resonance mode with an eigenfrequency of about 800 Hz becomes pronounced as the size of the hole is increased, posing problems for velocity sensing at higher frequencies. This mode may be related to inflation of the bellows. It is likely that its eigenfrequency can be increased by use of metal bellows, yet preserving the same axial stiffness of the bellows. A study of this option is planned for the future.

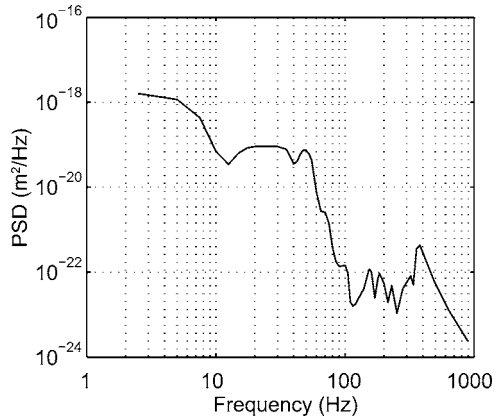

Fig. 18 Sensor noise power spectral density.

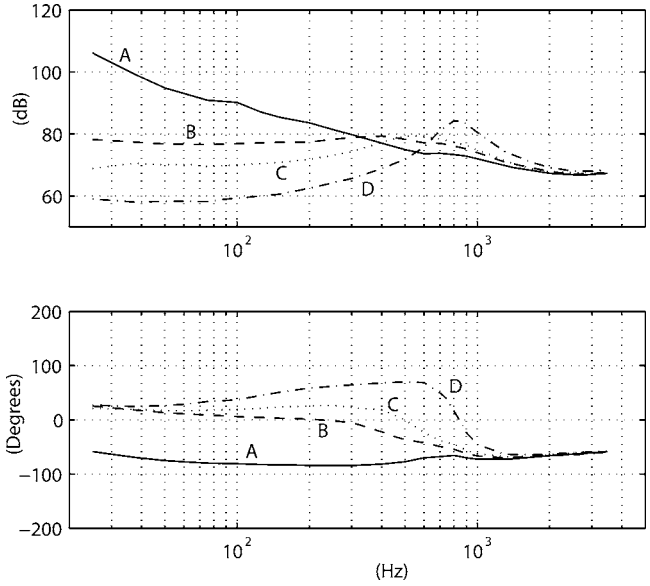

Fig. 19 Frequency response of the device used as a velocity sensor with a hole in the bellows. Input: faceplate velocity; output: microphone signal. A: no hole; B: 0.5-mm^2 hole; C: 1.5-mm^2 hole; D: 3-mm^2 hole (all values approximate).

6 Global Control

Design of a global mirror controller with thousands of inputs and outputs, and hundreds of structural eigenfrequencies inside the bandwidth, is highly challenging. In principle, it is possible to establish a MIMO controller with full control matrices. In practice, however it is not easy, so the task is broken down into forming many parallel control systems, each controlling only one actuator or a small family of actuators.

6.1 *Mirror Models*

A finite element model of the Euro50 secondary mirror was formulated in Ansys. The model takes composite lamination and anisotropic effects of CFRP into account using SHELL181 elements. There are 448,008 degrees of freedom (dof) and 74,266 elements. A modal decomposition was performed. The lowest 2,000 eigenfrequencies are shown in Fig. 20. There are 820 frequencies below 500 Hz, the minimum acceptable bandwidth of the DM control system. Figure 21 shows four of the eigenmodes. The mirror has a fixed support ring at its center, and the distance between the actuators (arranged in a hexagonal pattern) is 69 mm for K-band operation.

A first model reduction was established using modal truncation, simply retaining only the modes corresponding to the 2002 lowest eigenfrequencies. This model was in some cases not precise enough for control system simulation, so a second model was also derived by Guyan reduction of the finite element model. The principle is to discard those dof that have no input forces associated to them and little mass or moment of inertia. Statically, such a model is as precise as the full model, but dynamically, the omission of nodes involves an approximation. The reduced model

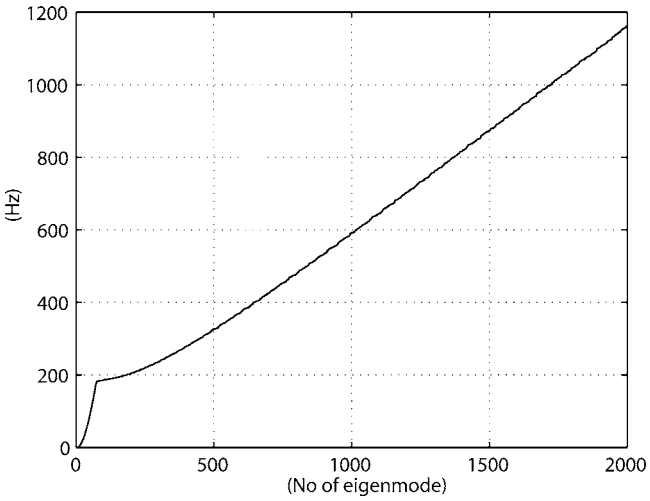

Fig. 20 Lowest 2000 eigenfrequencies versus eigenmode number.

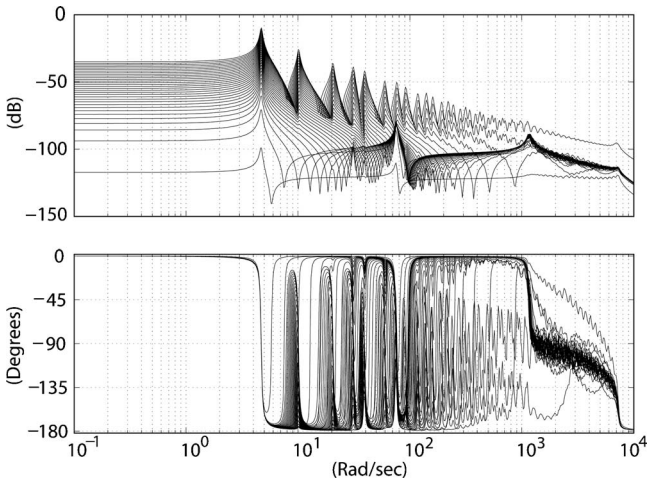

Fig. 22 Bode plots of transfer functions from actuator force, F_a, to displacement, x_m, at the same location for representative actuators at different locations over the mirror.

has 3354 dof with eigenfrequencies in the range 0.75 to 6196 Hz. The corresponding state-space model has 6708 state variables.

For design of the global control system of the DM, a reduced model involving one actuator with two rings of actuators around it in a hexagonal pattern (altogether 19 dof) was deduced by the Rayleigh-Ritz method. The 3354-dof model was loaded with unit forces at the 19 nodes of interest, and the corresponding static deflection patterns were applied as approximated eigenmodes for the Rayleigh-Ritz reduction.[19] The corresponding eigenfrequencies lie in the range 2.7 to 3630 Hz. More details on this model are given in Sec. 6.3.

6.2 *SISO Control*

The option of using one SISO controller for each of the actuators to control faceplate deflection was studied. For an introductory study we assumed mirror deflection sensors to be collocated with the actuators and disregarded actuator and sensor dynamics.

Transfer functions (from actuator force F_a to mirror deformation x_m at the same position) for each of the actuators were derived from the truncated model with 2002 eigenmodes, and some of these can be seen in Fig. 22. The shape of the transfer functions depends on the location of the actuator on the mirror. The transfer functions can be divided into six families with similar dynamics, so individual compensation filters were designed for each family, using a variety of lead, lag, and notch filters. Simulations with the Guyan mirror model using the SISO control approach for each of the actuators showed that, although the individual actuators were stable, the global system was unstable due to cross-coupling between the SISO loops. Methods for suppression of crosstalk to create a stable global system are the subject of the next section.

A SISO approach with *electronic damping* has been shown to work for the Large Binocular Telescope (LBT).[3,4,20,21] However, use of electronic damping limits the bandwidth achievable,[6] so the target bandwidth of the LBT was only 200 Hz for a much smaller mirror than for the Euro50 described. Hence, it is desirable to study methods for achieving a higher bandwidth.

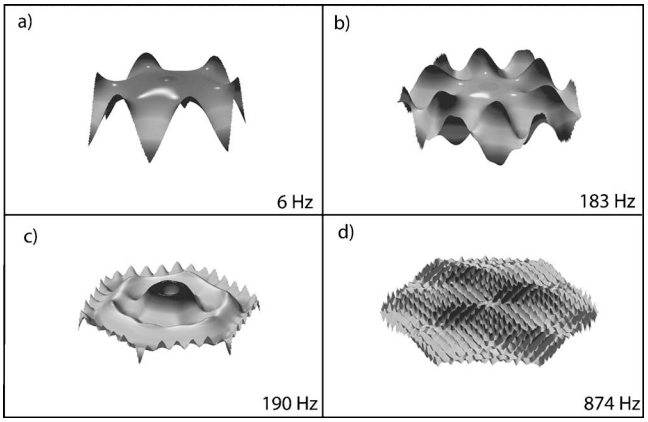

Fig. 21 Four eigenmodes of the Euro50 deformable mirror.

6.3 *Local MIMO Control*

MIMO approaches can be used to suppress crosstalk between actuators. In a hierarchy, a global regulator controls many local regulators, each involving two rings of actuators around a central one. The objective of the central actuator is to deflect the mirror as desired, whereas that of the actuators in the two rings is to suppress the influence from the central actuator outside it. For any actuator, an entire family of 18 actuators around it must be controlled, so (disregarding edge effects) there are in total 3168 MIMO control systems working in parallel, each controlling 19 actuators. The control signals from all MIMO controllers are superimposed, and each actuator receives a superimposed input from 19 MIMO controllers.

To suppress deflection outside the central actuator, a reduced mirror model derived by the Rayleigh-Ritz approach as described in Sec. 6.1 is used. The reduced system is described by the second-order differential equations

$$\mathbf{M}\ddot{\mathbf{x}} + \mathbf{C}\dot{\mathbf{x}} + \mathbf{K}\mathbf{x} = \mathbf{f},$$

where $\mathbf{K}$ is the stiffness matrix of the reduced system; $\mathbf{C}$ the damping matrix; $\mathbf{x}$ the mirror deflections of the 19 mirror points arranged in a vector with the one in the center as number 1, the inner ring as numbers 2 to 7, and the outer ring as numbers 9 to 19; and $\mathbf{f}$ is the corresponding actuator force vector. Assuming mass-normalized eigenvectors stored in columns of a matrix $\mathbf{\Phi}$, and a noncomplex modal damping, the transformation $\mathbf{q}=\mathbf{\Phi}^T\mathbf{x}$ gives

$$\ddot{\mathbf{q}} + 2\mathbf{Z}\mathbf{\Omega}\dot{\mathbf{q}} + \mathbf{\Omega}^2\mathbf{q} = \mathbf{\Phi}^T\mathbf{f},$$

with $\mathbf{\Omega}=\mathrm{diag}(\omega_1, \omega_2, \ldots, \omega_{19})$ and $\mathbf{Z}=\mathrm{diag}(\zeta_1, \zeta_2, \ldots, \zeta_{19})$, where ω_i is the eigenfrequency and ζ_i the damping ratio for the i'th mode. The modal coordinates $\mathbf{q}$ are mutually decoupled. Transformation to a state-space model with

$$\mathbf{z} = \begin{Bmatrix} \mathbf{q} \\ \dot{\mathbf{q}} \end{Bmatrix}$$

gives the system of first-order equations defining $\mathbf{A}$, $\mathbf{B}$, and $\mathbf{C}$:

$$\dot{\mathbf{z}} = \mathbf{A}\mathbf{z} + \mathbf{B}\mathbf{f} = \begin{Bmatrix} \mathbf{0} & \mathbf{I} \\ -\mathbf{\Omega}^2 & -2\mathbf{Z}\mathbf{\Omega}^2 \end{Bmatrix}\mathbf{z} + \begin{Bmatrix} \mathbf{0} \\ \mathbf{\Phi}^T \end{Bmatrix}\mathbf{f},$$

$$\mathbf{x} = \mathbf{C}\mathbf{z} = \{\mathbf{\Phi}\ \mathbf{0}\}\mathbf{z}. \tag{1}$$

This system is of order 38 and readily usable for design of local controllers. Simulations with the full model have shown that it is necessary to dampen modes of the local system to achieve satisfactory global stability. Hence, a modal controller was used, increasing damping for significant local model modes. Three of them have circular symmetry (the only ones with this feature), and one does not. Modes with circular symmetry are globally significant because the symmetrical force pattern excites symmetrical eigenmodes.

The corresponding local modal velocities were fed back to a proportional regulator that controls the actuators after a transformation from modal to nodal coordinates. The actuator force commands for the i'th mode (equation 1) are

$$\mathbf{f}_i = \boldsymbol{\psi}_i \rho_i \cdot q_i,$$

where ψ_i is the i'th eigenvector arranged in a column, and ρ_i is the proportional gain of the modal damping loop for eigenmode i.

Figure 23 shows Bode plots of local transfer functions from the center actuator force to the deformation at the same location. The transfer function, (a), is the original SISO open-loop function. The second transfer function, (b), has local modal control added, thereby eliminating the high-frequency resonance peaks.

A study of the full system with modal damping and all parallel control loops is in progress, together with the establishment of observers to provide the modal velocities. The advance is somewhat slow, due to the long simulation times (weeks). Early simulations with equal nodal velocity gains (i.e., different modal gains) have shown that a global bandwidth of 800 Hz is within reach.

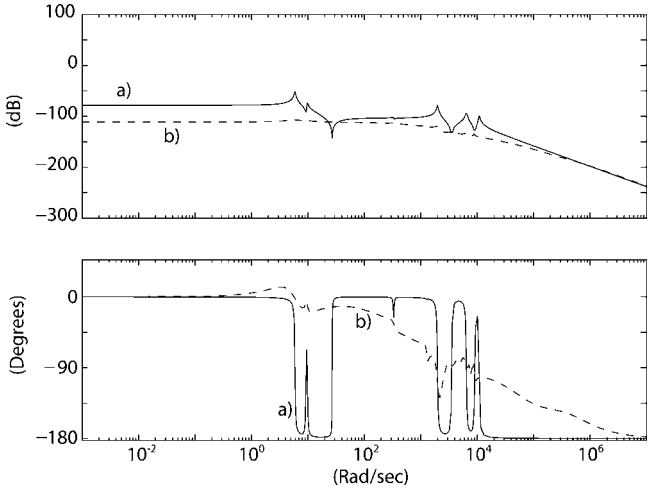

Fig. 23 Transfer functions from center actuator force to deformation at the same location: (a) SISO open-loop, (b) system with modal damping.

Realistic DM command signals were generated using the full integrated model of the Euro50 to test whether the 80-nm rms limit for K-band operation can be achieved with the local nodal damping model. The results were unsatisfactory on the mirror edges, but when three edge rings are excluded from the calculation of the surface accuracy, the total DM form error is 3.2 nm rms, indicating that the specifications were met for these actuator positions. This confirms the criticality of the edge control and this issue will be studied in future research.

7 Conclusions and Further Work

Design and construction of a 4-m DM with a bandwidth of 500 to 1000 Hz is a challenge from a feasibility and cost point of view. Our studies suggest that new approaches may be attractive. Actuators with internal feedback allow use of suction cups, seemingly a prerequisite for affordable construction of large DMs with thousands of actuators. Novel mirror deflection sensors costing about $10 and based on electret microphones provide a resolution in the 10- to 20-nm range. For global control of the mirror, parallel local controllers with modal damping based on local observers for families of actuators may be attractive.

A prototype of a single actuator and a mirror simulator were built, and a variety of tests carried out. More experiments are needed before an ELT DM can be built, and work is in progress. For the near future, a laboratory test prototype with 7 or 19 actuators has high priority. In addition, closer studies and optimization of the electret-microphone-based sensor will be undertaken to achieve an even larger bandwidth and smaller dimensions, and simulations of the global control of the full mirror and the laboratory prototype will be made.

Acknowledgments

We thank Anders Robertsson from the Department of Automatic Control, and Gustaf Olsson from the Department of Industrial Electrical Engineering and Automation, both of Lund Institute of Technology, Sweden, for participation in the project. We are grateful for the support from Torben

Licht, Bruel & Kjaer, Denmark, who lent us a laser velocimeter and vibration measuring equipment, and to Henrik Thrane, Ødegaard & Danneskiold-Samsøe, Denmark, for advice on microphones. Finally, we thank Holger Riewaldt, Lund Observatory, for the mechanical design, and Nels Hansson, Lund Observatory, for helping us with the test stand. This work was carried out with support from the Royal Physiographic Society, Sweden.

References

1. J. Beckers, in "NOAO proposal to NSF for 8 m telescopes," Appendix N, Tech. Rep., NOAO (1989).
2. G. Brusa, A. Riccardi, M. Accardo, V. Biliotti, M. Carbillet, C. D. Vecchio, S. Esposito, B. Femenia, O. Feeney, L. Fini, S. Gennari, L. Miglietta, P. Salinari, and P. Stefanini, "From adaptive secondary mirrors to extra-thin extra-large adaptive primary mirrors," in *Bäckaskog Workshop on Extremely Large Telescopes*, T. Andersen, A. Ardeberg, and R. Gilmozzi, Eds., *ESO Conf. Workshop Proc.* **57**, 181–201 (1999).
3. F. Wildi, G. Brusa, A. Riccardi, M. Lloyd-Hart, H. Martin, and L. Close, "Towards 1st light of the 6.5m MMT adaptive optics system with deformable secondary mirror," in *Adaptive Optical System Technologies II*, P. Wizinowich and D. Bonaccini, Eds., *Proc. SPIE* **4839**, 155–163 (2003).
4. A. Riccardi, G. Brusa, C. D. Vecchio, R. Biasi, M. Andrighettoni, D. Gallieni, F. Zocchi, M. Lloyd-Hart, H. M. Martin, and F. Wildi, "The adaptive secondary mirror for the 6.5m conversion of the Multiple Mirror Telescope," in *Beyond Conventional Adaptive Optics*, E. Vernet, R. Ragazzoni, S. Esposito, and N. Hubin, Eds., *ESO Conf. Workshop Proc.* **58**, 55–64 (2001).
5. D. W. Miller and S. C. O. Grocott, "Robust control of the Multiple Mirror Telescope adaptive secondary mirror," *Opt. Eng.* **38**, 1276–1287 (Aug. 1999).
6. S. C. O. Grocott, "Dynamic reconstruction and multivariable control for force-actuated, thin facesheet adaptive optics," PhD Thesis, Massachusetts Institute of Technology (1997).
7. J. H. Lee, B. C. Bigelow, D. D. Walker, A. P. Doel, and R. G. Bingham, "Why adaptive secondaries?," *Publ. Astron. Soc. Pac.* **112**, 97–107 (Jan. 2000).
8. P. Doel, S. Kendrew, D. Brooks, C. Dorn, C. Yates, R. D. Martin, I. Richardson, and G. Evans, "Development of an active carbon fibre composite mirror," in *Advancements in Adaptive Optics*, D. Bonaccini, B. Ellerbroek, and R. Ragazzoni, Eds., *Proc. SPIE* **5490**, 1526–1533 (2004).
9. S. Kendrew and P. Doel, "Finite element analysis of carbon fibre composite adaptive mirrors," in *Advancements in Adaptive Optics*, D. Bonaccini, B. Ellerbroek, and R. Ragazzoni, Eds., *Proc. SPIE* **5490**, 1591–1599 (2004).
10. T. Andersen, M. Owner-Petersen, and A. Ardeberg Eds., *Euro50: Design Study of a* 50 m *Adaptive Optics Telescope*, Lund Observatory (2003).
11. P. C. Chen, C. W. Bowers, D. A. Content, M. Marzouk, and R. C. Romeo, "Advances in very lightweight composite mirror technology," *Opt. Eng.* **39**, 2320–2329 (Aug. 2000).
12. H. E. Bennett, R. C. Romeo, J. J. Shaffer, and P. C. Chen, "Development of lightweight mirror elements for the Euro50 mirrors," in *Emerging Optoelectronic Applications*, G. E. Jabbour and J. T. Rantala, Eds., *Proc. SPIE* **5382**, 526–532 (2004).
13. T. E. Andersen, A. Ardeberg, H. Riewaldt, M. Lastiwka, N. Quinlan, K. McNamara, X. Wang, A. Enmark, M. Owner-Petersen, A. Shearer, C. Fan, and D. Moraru, "Status of the Euro50 project," in *Ground-Based Telescopes*, J. M. Oschmann, Ed., *Proc. SPIE* **5489**, 407–416 (2004).
14. T. Andersen, M. Owner-Petersen, and H. Riewaldt, "Integrated simulation model of the Euro50," in *Integrated Modeling of Telescopes*, T. Andersen, Ed., *Proc. SPIE* **4757**, 84–92 (2002).
15. T. E. Andersen, A. Enmark, D. Moraru, C. Fan, M. Owner-Petersen, H. Riewaldt, M. Browne, and A. Shearer, "A parallel integrated model of the Euro50," in *Modeling and Systems Engineering for Astronomy*, S. C. Craig and M. J. Cullum, Eds., *Proc. SPIE* **5497**, 251–265 (2004).
16. G. Ellis and R. Lorenz, "Resonant load control methods for industrial servo drives," in *IEEE-IAS Conf. Recs, IEEE-IAS*, Vol **3**, 1438–1445, IEEE (2000).
17. J. W. Hardy, *Adaptive Optics for Astronomical Telescopes*, Oxford Univ. Press (1998).
18. T. Andersen, "Vibration sensor," Patent application 35316 (2005).
19. J. T. Spanos and W. S. Tsuha, "Selection of component modes for flexible multibody simulation," *J. Guid. Control* **14**, 278–283 (Mar.-Apr. 1991).
20. A. Riccardi, G. Brusa, M. Xompero, D. Zanotti, C. D. Vecchio, P. Salinari, P. Ranfagni, D. Gallieni, R. Biasi, M. Andrighettoni, S. Miller, and P. Mantegazza, "The adaptive secondary mirrors for the Large Binocular Telescope: a progress report," in *Advancements in Adaptive Optics*, D. Bonaccini, B. Ellerbroek, and R. Ragazzoni, Eds., *Proc. SPIE* **5490**, 1564–1571 (2004).
21. A. Riccardi, G. Brusa, P. Salinari, S. Busoni, O. Lardiere, P. Ranfagni, D. Gallieni, R. Biasi, M. Andrighettoni, S. Miller, and P. Mantegazza, "Adaptive secondary mirrors for the Large Binocular Telescope," in *Astronomical Adaptive Optics Systems and Applications*, R. K. Tyson and M. Lloyd-Hart, Eds., *Proc. SPIE* **5169**, 159–168 (2003).

Torben Andersen has a PhD in control engineering. From 1974 to 1979 he was in charge of the design of the Coudé Auxiliary Telescope at European Southern Observatory in Geneva. Subsequently he worked with steerable shipborne antennas for a few years. From 1984 to 1994 he was head of engineering for the Nordic Optical Telescope Scientific Association that built the Nordic Optical Telescope on La Palma and designed the 32-m EISCAT antenna on Spitsbergen. From 1994 to 1997 he was first head of systems engineering and later also head of telescope engineering for the VLT division of the European Southern Observatory. In 1997 he became a professor of optomechanical design at the Institute of Astronomy, Lund University, Sweden, and he is one of the architects behind Euro50, a proposed 50-m optical telescope with adaptive optics.

Olof Garpinger graduated in 2005 at Lund Institute of Technology with a MSc in engineering physics and, together with a colleague, carried out his diploma project on the control of large DMs. He is now a postgraduate student in the field of automatic control.

Mette Owner-Petersen graduated in electro-physics engineering from the Technical University of Denmark (DTU) in 1967. In 1970 she received her PhD degree for the work "Cyclotron resonance in Si with special regard to quantum effects in the valence band" from the same university. From 1970 to 2000 she was a lecturer at the Physics Institute at DTU, teaching elementary-particle and nuclear physics, laser techniques, holography, and optics, and doing research in laser construction, Stark spectroscopy, and digital speckle interferometry. From 1991 to 1995 she worked for Nordic Telescope Group, concentrating on optical design of extremely large telescopes (ELTs) and instrumentation for the planned solar telescope LEST. Since 2000 she has held a position as lecturer at Lund Observatory, continuing her work with ELTs, and has participated in the European collaboration for a 50-m adaptive optics telescope, Euro50. The main area of her work is related to multiconjugate adaptive optics.

Fredrik Bjoorn graduated in 2005 at Lund Institute of Technology with a MSc in electronic engineering and, together with a colleague, carried out his diploma project on the control of large deformable mirrors.

Roger Svahn graduated in 2005 at Lund Institute of Technology with a MSc in electronic engineering and carried out his diploma project on the design of actuators for large deformable mirrors.

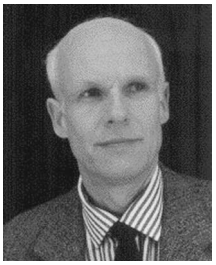

Arne Ardeberg graduated in mathematics and physics in 1964 and obtained his PhD degree in 1973 in astrophysics, both at Lund University, Sweden. In 1980, he was appointed professor of astronomy and astrophysics at the Department of Astronomy, Lund University. From 1969 to 1973, he served as staff astronomer of the European Southern Observatory (ESO) in Chile. Between 1979 and 1984, he was the Director of ESO in Chile. From 1984 and until 1995, he was the Director of the Nordic Optical Telescope (NOT) Scientific Association, constructing and operating NOT on La Palma, Canary Islands. Between 1998 and 2003, he was vice president of Lund University. Since 2004, he has been the director of the Department of Astronomy, Lund University. Since 1991, he has been involved in the Euro50 project.